Commun. Comput. Phys.
doi: 10.4208/cicp.090410.260410a

Vol. **9**, No. 2, pp. 231-239
February 2011

Improved Unlike-Particle Collision Operator for delta-f Drift-Kinetic Particle Simulations

R. A. Kolesnikov[1,*], W. X. Wang[2] and F. L. Hinton[3]

[1] *Los Alamos National Laboratory, Los Alamos, NM 87544, USA.*
[2] *Plasma Physics Laboratory, P.O. Box 451, Princeton, NJ 08543, USA.*
[3] *Center for Astrophysics & Space Science, University of California, San Diego, La Jolla, CA 92093, USA.*

Received 9 April 2010; Accepted (in revised version) 26 April 2010

Communicated by Xueqiao Xu

Available online 27 August 2010

Abstract. Plasmas in modern tokamak experiments contain a significant fraction of impurity ion species in addition to main deuterium background. A new unlike-particle collision operator for δf particle simulation has been developed to study the non-local effects of impurities due to finite ion orbits on neoclassical transport in toroidal plasmas. A new algorithm for simulation of cross-collisions between different ion species includes test-particle and conserving field-particle operators. An improved field-particle operator is designed to exactly enforce conservation of number, momentum and energy.

PACS: 52.30.Gz, 52.25.Xz, 52.25.Dg

Key words: Drift-kinetics, magnetized plasmas.

1 Introduction

To understand the performance of fusion toroidal devices in improved confinement regime when the turbulent transport is reduced in the ion channel, the experimental data is compared with neoclassical transport level. Neoclassical theory has been well developed [1–3] to understand this irreducible transport in local small ion orbit limit. And a direct numerical solution of the drift kinetic equations globally is needed to address non-local features of the dynamics [4–6] near magnetic axis or sharp profile gradients where basic assumptions of most local theories are violated. In addition to main ion species, which is normally deuterium, most of experimentally relevant plasmas contain one or

*Corresponding author. *Email addresses:* rkolesni@lanl.gov (R. A. Kolesnikov), wwang@pppl.gov (W. X. Wang), fhinton@ucsd.edu (F. L. Hinton)

 ©2011 Global-Science Press

more ion species. Consequently, impurity particles can make a significant contribution to main deuterium heat flux indirectly by producing additional cross-species collisions. In this paper we address the development of an unlike-particle collision operator for δf particle simulation technique. In addition to a test-particle operator, we describe a new field-particle operator which conserves particle number, energy and momentum.

The distribution function $F_s(\boldsymbol{X},t)$ species s (with mass m_s and charge Z_s) evolves according to the drift-kinetic equation

$$\frac{D}{Dt}F_s \equiv \left(\frac{\partial}{\partial t}+\dot{\boldsymbol{X}}\cdot\frac{\partial}{\partial \boldsymbol{X}}\right)F_s = \sum_b C_{sb}[F_a,F_b]. \tag{1.1}$$

The operator on the right hand side describes self-collisions of species s as well as cross-collisions between various species. The guiding center coordinates $\boldsymbol{X}=(\boldsymbol{x},\rho_{||},\mu)$ evolve according to the Lagrangian equations

$$\frac{d}{dt}\left(\frac{\partial}{\partial \dot{\boldsymbol{X}}}L_s\right)-\frac{\partial}{\partial \boldsymbol{X}}L_s=0. \tag{1.2}$$

Here L_s is Lagrangian and $\boldsymbol{x}=(r,\theta,\zeta)$ where r, θ and ζ are radial, poloidal and toroidal spatial coordinates correspondingly. The magnetic moment $\mu=m_s v_\perp^2/2B$ ($\dot{\mu}=0$ due to conservation of the adiabatic moment) and parallel gyroradius $\rho_{||}=m_s v_{||}/Z_s eB$ are expressed in terms of parallel and perpendicular velocities $v_{||}$ and $v_\perp$.

The δf algorithm [4,7,8] involves solving the following equation

$$\frac{D}{Dt}\delta f_s = -\dot{\boldsymbol{X}}\cdot\frac{\partial}{\partial \boldsymbol{X}}F_{0s}+\sum_b\Big(C_{sb}[\delta f_s,F_{0b}]+C_{sb}[F_{0s},\delta f_b]\Big), \tag{1.3}$$

which is obtained directly from Eq. (1.1) by substituting $F_s=F_{0s}+\delta f_s$ and linearising the collision operator. F_{0s} is a time-independent shifted Maxwellian distribution function which satisfies $C_{sb}[F_{0s},F_{0b}]=0$ for any s and b.

The local shifted Maxwellian background distribution function is written in the following form [4,9]

$$F_{0s}\equiv F_{0s}(n_s,T,U_\parallel)=n_s\left(\frac{m_s}{2\pi T}\right)^{3/2}\exp\Big[-\frac{m_s}{T}\left((v_\parallel-U_\parallel)^2/2+\mu B\right)\Big]. \tag{1.4}$$

Here $n_a(r)\equiv\langle n_a(r,\theta)\rangle$, $T(r)$ and $\omega_t(r)=[B/I(r)]U_\parallel(r,\theta)$ are experimentally given profiles for the ion density, temperature and toroidal angular frequency. $I(r)=RB_\zeta$, where R is the major radius, B_ζ and B_θ are the toroidal and poloidal components of the magnetic field $\boldsymbol{B}$.

Since the constraint $C_{sb}[F_{0s},F_{0b}]=0$ on background Maxwellian distribution functions must be satisfied, one need to have the same ion temperature $T(r)$ and parallel flow $U_\parallel(r)$ profiles in the distribution functions (1.4) for all species. The difference between experimentally observed temperatures $T_s(r)$ and toroidal angular frequencies $\omega_{ts}(r)$ between different species is captured by initial $\delta f_s(t=0)$ in the following form

$$\delta f_s(t=0)=F_{0s}(n_s,T_s,U_{||s})-F_{0s}(n_s,T,U_{||}). \tag{1.5}$$

Our δf algorithm with linearized collision operator requires that $\delta f_s / F_{0s} \ll 1$. While temperature and parallel velocity profiles may be substantially different between different species, especially between ions and electrons, recent drift-kinetic simulations of realistic axisymmetric toroidal fusion devices show that this condition is well satisfied in deuterium plasmas in presence of carbon impurity [5, 6].

The two-weight algorithm [10] assigns weights $w \sim \delta f_s / F_{0s}$ and $1-p \sim g_s / F_{0s}$ to each simulation marker. Here the marker distribution function g_s for species s in the extended phase space is defined as follows

$$g_s(\boldsymbol{X},w,p,t) \sim \sum_i \delta(\boldsymbol{X}-\boldsymbol{X}_{si}(t))\delta(w-w_{si}(t))\delta(p-p_{si}(t)), \tag{1.6}$$

The need for the second weight p is motivated by the fact that in neoclassical simulations marker distribution function might also significantly deviate from the background F_{0s}.

The kinetic equation for g_s is

$$\frac{Dg_s}{Dt} + \frac{\partial}{\partial p}\left(\frac{dp}{dt}g_s\right) + \frac{\partial}{\partial w}\left(\frac{dw}{dt}g_s\right) = \sum_b C_{ab}[g_s, F_{0b}]. \tag{1.7}$$

Eq. (1.3) for the evolution of δf_s as well as trivial equation for the background distribution function $DF_{0s}/Dt = 0$ are reproduced when the following definitions for the marker particle weights w and p are adopted

$$\int dwwdpg_s = \delta f_s, \tag{1.8a}$$

$$\int dwdp(1-p)g_s = F_{0s} \tag{1.8b}$$

together with the following equations of motion for the two marker weights

$$\frac{dw}{dt} = \frac{1-p}{F_{0s}}\left(-\frac{DF_{0s}}{Dt} + \sum_b C_{sb}[F_{0s}, \delta f_b]\right) - \eta(w-\overline{w}_s), \tag{1.9a}$$

$$\frac{dp}{dt} = \frac{1-p}{F_{0s}}\left(-\frac{DF_{0s}}{Dt}\right) - \eta(p-\overline{p}_s). \tag{1.9b}$$

Here η is the damping rate [11], which provides a continuous relaxation of w and p toward their locally average values $\overline{w}_s$ and $\overline{p}_s$. This procedure is introduced to reduce particle noise due to marker weight spreading without affecting physics results. Equations for δf_s and F_{0s} are not affected by these additional terms, which may be illustrated by substituting Eqs. (1.9a)-(1.9b) into Eq. (1.7) and taking moments Eqs. (1.8a)-(1.8b).

2 Operator for unlike-particle collisions

The linearised unlike-particle collision operator for species a colliding with species b can be rewritten as follows

$$C_{ab}[\delta f_a, F_{0b}] + C_{ab}[F_{0a}, \delta f_b] \equiv C_{ab}^{TP}(\delta f_a) + C_{ab}^{FP}(\delta f_b), \tag{2.1}$$

where the test-particle operator

$$C_{ab}^{TP}(\delta f_a)=\frac{\partial}{\partial \boldsymbol{v}}\cdot(\boldsymbol{v}F\delta f_a)+\frac{\partial^2}{\partial \boldsymbol{v}\partial \boldsymbol{v}}:\left(G\boldsymbol{I}+H\frac{\boldsymbol{vv}}{v^2}\right)\delta f_a \tag{2.2}$$

describes the drag and diffusion. The coefficients

$$F=-\nu_{ab}\frac{v^3}{n_b}\frac{\partial}{\partial \boldsymbol{v}}H_b(\boldsymbol{v}), \tag{2.3a}$$

$$G=\nu_{ab}\frac{v^2}{2n_b}\frac{\partial}{\partial v}G_b(\boldsymbol{v}), \tag{2.3b}$$

$$H=\nu_{ab}\frac{v^3}{2n_b}\left(\frac{\partial^2}{\partial v^2}-\frac{1}{v}\frac{\partial}{\partial v}\right)G_b(\boldsymbol{v}) \tag{2.3c}$$

are expressed in terms Rosenbluth's potentials

$$G_b(\boldsymbol{v})=\int d^3v' F_{0b}(v')|\boldsymbol{v}-\boldsymbol{v}'|, \tag{2.4a}$$

$$H_b(\boldsymbol{v})=\left(1+\frac{m_a}{m_b}\right)\int d^3v'\frac{F_{0b}(v')}{|\boldsymbol{v}-\boldsymbol{v}'|}. \tag{2.4b}$$

Here the collision frequency is defined by $\nu_{ab}=4\pi Z_a^2 Z_b^2\Lambda_{ab}n_b/m_a^2v_a^3$. The standard Monte Carlo technique [12] is utilized in the drift-kinetic simulation to implement this operator.

The field-particle operator appears as a source term in Eq. (1.3), and not being sensitive to the details of δf_b, may be rewritten in the following form [13, 14]

$$C_{ab0}^{FP}(\delta f_b)=\mathcal{R}_{ab}(v)v_\parallel\delta P_{ab}^0+\mathcal{Q}_{ab}(v)\delta E_{ab}^0. \tag{2.5}$$

The number, momentum and energy lost by species b test particles as a result of collisions with species a field particles are

$$\delta N_{ab}^0=-\int d^3v C_{ba}^{TP}(\delta f_b)=0, \tag{2.6a}$$

$$\delta P_{ab}^0=-\int d^3v m_b v_\parallel C_{ba}^{TP}(\delta f_b), \tag{2.6b}$$

$$\delta E_{ab}^0=-\int d^3v (m_b v^2/2) C_{ba}^{TP}(\delta f_b). \tag{2.6c}$$

The functions $\mathcal{R}_{ab}$ and $\mathcal{Q}_{ab}$ are to be determined from the requirement that momentum and energy gained by species a field particles must equal that lost by species b test particles

$$\int d^3v m_a v_\parallel C_{ab}^{FP}(\delta f_b)=\delta P_{ab}^0, \tag{2.7a}$$

$$\int d^3v (m_a v^2/2) C_{ab}^{FP}(\delta f_b)=\delta E_{ab}^0. \tag{2.7b}$$

With appropriate choices of multiplying factors, the functions $\mathcal{R}_{ab}$ and $\mathcal{Q}_{ab}$ may be found as follows:

$$\mathcal{R}_{ab}(v)v_{\|}=\frac{C_{ab}^{TP}(m_a v_{\|}F_{0a})}{\int d^3v' m_a v'_{\|}C_{ab}^{TP}(m_a v'_{\|}F_{0a})}, \tag{2.8a}$$

$$\mathcal{Q}_{ab}(v)=\frac{C_{ab}^{TP}(m_a v^2 F_{0a})}{\int d^3v'(m_a v'^2/2)C_{ab}^{TP}(m_a v'^2 F_{0a})}. \tag{2.8b}$$

The resulting operator Eq. (2.5) now satisfies conservation properties Eqs. (2.7a)-(2.7b). This can be verified by remembering that the test-particle operator preserves parity in $v'_{\|}$. Specifically, $C_{ab}^{TP}(m_a v'_{\|}F_{0a})$ is odd in $v'_{\|}$, and $C_{ab}^{TP}(m_a v'^2 F_{0a})$ is even in $v'_{\|}$.

Since we use Maxwellian background distribution functions, these expressions may be simplified by analytically computing the Rosenbluth potentials [12]:

$$\mathcal{R}_{ab}(v)=\frac{3\sqrt{\pi}}{4n_a T}(1+m_b/m_a)^{3/2}y_b^{-3/2}\phi(y_b), \tag{2.9a}$$

$$\mathcal{Q}_{ab}(v)=\frac{\sqrt{\pi}}{2n_a T}(1+m_b/m_a)^{3/2}y_b^{-1/2}(m_a/m_b-d/dy_b)\phi(y_b), \tag{2.9b}$$

where $\phi(y)=2/\sqrt{\pi}\int_0^y e^t\sqrt{t}dt$ and $y_b=v^2/v_b^2$.

As was illustrated by Sugama *et al.* [15], the test-particle C_{ab}^{TP} and field-particle C_{ab0}^{FP} operators defined by Eq. (2.5) and (2.5) satisfy the adjointness relations

$$\int d^3v\frac{\delta f_a}{F_{0a}}C_{ab}^{TP}(\delta g_a)=\int d^3v\frac{\delta g_a}{F_{0a}}C_{ab}^{TP}(\delta g_a), \tag{2.10a}$$

$$\frac{T_a}{T_b}\int d^3v\frac{\delta f_a}{F_{0a}}C_{ab0}^{FP}(\delta f_b)=\int d^3v\frac{\delta f_b}{F_{0b}}C_{ba0}^{FP}(\delta f_a), \tag{2.10b}$$

as well as Boltzmann's H-theorem

$$\begin{aligned}\frac{T_a}{T_b}\int d^3v\frac{\delta f_a}{F_{0a}}[C_{ab}^{TP}(\delta f_a)+C_{ab}^{FP}(\delta f_b)]\\ +\int d^3v\frac{\delta f_b}{F_{0b}}[C_{ba}^{TP}(\delta f_b)+C_{ba}^{FP}(\delta f_a)]\leq 0,\end{aligned} \tag{2.11}$$

which states the asymptotic relaxation of the distribution function to the local Maxwellian equilibrium state.

In Eq. (2.11), the left hand side vanishes when δf_s perturbations in the following form

$$\delta f_s=F_{0s}\left[\frac{\delta n_s}{n_s}+\frac{m_s}{T_s}\delta U_{\|}v_{\|}+\frac{\delta T_s}{T_s}\left(\frac{m_a v^2}{2T_a}-\frac{3}{2}\right)\right] \tag{2.12}$$

satisfy the correct null space of the linearized operator

$$C_{ab}^{TP}(\delta f_a)+C_{ab}^{FP}(\delta f_b)=0. \tag{2.13}$$

Implementation of C^{FP}_{ab0} according to (2.5) within δf algorithm Eqs. (1.9a)-(1.9b) leads to unsatisfactory particle number conservation properties. This is due to the fact that, although test-particle operator conserves number according to Eq. (2.6a), the field-particle operator Eq. (2.5) affects particle number moment $\int d^3v\delta f$ by altering δf according to Eq. (1.3). To obtain improved field-particle operator, one can use the procedure developed by Wang *et al.* [10] for iterative calculation of the field-particle conserving part in the following form

$$C^{FP}_{ab}(\delta f_b)=\sum_{n=0}^{N-1} C^{FP}_{abn}(\delta f_b), \tag{2.14a}$$

$$C^{FP}_{abn}(\delta f_b)=\mathcal{H}_{ab}(v)\delta N^n_{ab}+\mathcal{R}_{ab}(v)v_{\|}\delta P^n_{ab}+\mathcal{Q}_{ab}(v)\delta E^n_{ab}. \tag{2.14b}$$

An additional function $\mathcal{H}_{ab}$ is to be determined.

Operator (2.14a) is implemented as a sequence of N iterations to enforce the appropriate conservation constraints. Specifically, the first $n=0$ iteration enforces momentum and energy conservation according to Eqs. (2.7a)-(2.7b). Since simulation uses a finite number of markers, the consequent iterations are necessary to further improve momentum and energy (together with number) conservation properties according to

$$\delta N^n_{ab}=\int d^3v C^{FP}_{abn-1}(\delta f_b), \tag{2.15a}$$

$$\delta P^n_{ab}=\int d^3v m_b v_{\|} C^{FP}_{abn-1}(\delta f_b), \tag{2.15b}$$

$$\delta E^n_{ab}=\int d^3v (m_b v^2/2) C^{FP}_{abn-1}(\delta f_b). \tag{2.15c}$$

Analogously to $\mathcal{R}_{ab}$ and $\mathcal{Q}_{ab}$ functions, the $\mathcal{H}_{ab}$ function is chosen to be

$$\mathcal{H}_{ab}(v)=1-\mathcal{Q}_{ab}(v),$$

so that the resulting operator Eq. (2.14a) satisfies conservation properties Eqs. (2.15a)-(2.15c) as well as adjointness relation Eq. (2.10b) and H-theorem Eq. (2.11). Self-adjointness and H-theorem in presence of contribution in Eq. (2.14a) due to an additional $\mathcal{H}_{ab}(v)$ term can be demonstrated by remembering that the first ($n=0$) iteration enforces conservation of number and energy leading to

$$\delta N^1_{ab}\int d^3v \frac{\delta f_a}{F_{0a}}\mathcal{H}_{ab}(v)=0 \tag{2.16}$$

during the second ($n=1$) iteration.

3 Improved field-particle operator

Fig. 1 shows the residual errors in number and energy. The blue and the red crosses (for deuterium and carbon) show the errors due to application of $C^{FP}_{ab0}(\delta f_b)$ operator Eq. (2.5),

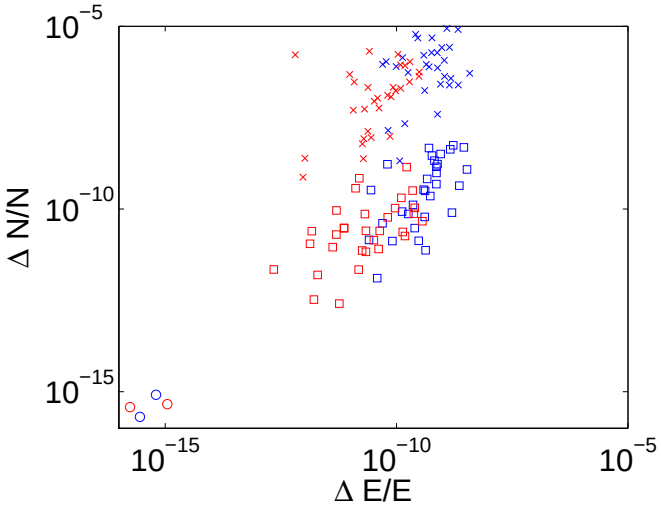

Figure 1: Residual errors in energy and number for a set of sample simulation markers. The blue and the red markers are for deuterium and carbon respectively.

which enforces conservation of only momentum and energy. The resulting error in particle number is not satisfactory, which is the reason $C_{ab}^{FP}(\delta f_b)$ operator (2.14a) needs to be used instead. Application of the complete operator (2.14a) leads to improved residual error in particle number, which is comparable to residual errors in momentum and energy (squares in Fig. 1). Three-time ($N=3$) recursive operations of C_{ab}^{FP} were used for this figure. Note that the deuterium component has slightly higher residual errors in all quantities compared to the carbon component due to higher thermal velocity.

While there is significant improvement in momentum and energy conservation when C_{ab}^{FP} is implemented, the residual errors will depend on the number of markers used in the simulation. It is difficult to have sufficient number of markers, especially for non-axisymmetric systems, for the error to converge. To resolve this problem, we follow the procedure developed by Satake [16] rewriting the field-particle operator in the following form

$$C_{ab}^{FP}(\delta f_b)=\mathcal{H}_{ab}(v)\delta N+\mathcal{R}_{ab}(v)v_{||}\delta P+\mathcal{Q}_{ab}(v)\delta E. \tag{3.1}$$

Instead of using theoretical values for the functions δN, δP and δE, we find them from solving the following equation

$$m_a\int d^3v\begin{pmatrix}1\\ v_{||}\\ v^2/2\end{pmatrix}C_{ab}^{FP}(\delta f_b)=\begin{pmatrix}\delta N_{ab}^0\\ \delta P_{ab}^0\\ \delta E_{ab}^0\end{pmatrix}, \tag{3.2}$$

which is a statement of conservation of number, momentum and energy Eqs. (2.6a)-(2.7b).

For the simulation with a finite number of markers, Eq. (3.2) may be rewritten as follows

$$\sum_{k=1}^{K}(1-p_k)\begin{pmatrix} \mathcal{H}_{ab} & \mathcal{R}_{ab}v_{\|} & \mathcal{Q}_{ab} \\ \mathcal{H}_{ab}v_{\|} & \mathcal{R}_{ab}v_{\|}^2 & \mathcal{Q}_{ab}v_{\|} \\ \mathcal{H}_{ab}v^2 & \mathcal{R}_{ab}v^2v_{\|} & \mathcal{Q}_{ab}v^2 \end{pmatrix}_k \times \begin{pmatrix} \delta N \\ \delta P \\ \delta E \end{pmatrix}$$
$$= -\begin{pmatrix} 0 \\ \delta P_{ab}^0/m_a \\ 2\delta E_{ab}^0/m_a \end{pmatrix}. \tag{3.3}$$

Eq. (3.3) is designed to precisely enforce conservation of number, momentum and energy locally in configuration space. k is the parameter to sum over the total number of markers K in a cell of a spatial grid. In this procedure, this spatial grid must be chosen to be fine enough to resolve the profiles of equilibrium magnetic field and radial electric field. Using this approach, the error is at the rounding-error level (circles in Fig. 1) for both deuterium and carbon, independent of the number of markers in the simulation.

4 Conclusions

The unlike-particle collision operator for δf gyrokinetic particle simulation is described. To study the neoclassical transport in toroidal plasmas, it is necessary to simulate the drift-kinetic equations in presence of electron and ion species using new operator. This operator includes test-particle and conserving field-particle parts. The improved version of the field-particle operator is designed to precisely enforce conservation of number, momentum and energy.

Acknowledgments

This work was supported by U.S. DOE Contract No. DE-AC02-09CH11466.

References

[1] F. L. Hinton and R. D. Hazeltine, Rev. Mod. Phys. 48 (1976) 239.
[2] S. P. Hirshman and D. J. Sigmar, Nucl. Fusion 21 (1981) 1079.
[3] P. Helander and D. J. Sigmar, Collisional Transport in Magnetized Plasmas, Chap. 12, Cambridge University Press, Cambridge, 2002.
[4] W. X. Wang, G. Rewoldt, W. M. Tang et al., Phys. Plasmas 13 (2006) 082501.
[5] R. A. Kolesnikov, W. X. Wang, F. L. Hinton, G. Rewoldt and W. M. Tang, PPCF 52 (2010) 042002.
[6] R. A. Kolesnikov, W. X. Wang, F. L. Hinton, G. Rewoldt and W. M. Tang, Phys. Plasmas 17 (2010) 022506.
[7] S. E. Parker and W. W. Lee, Phys. Fluids B 5 (1993) 77.
[8] W. W. Lee, Phys. Fluids 26 (1983) 556.

[9] F. L. Hinton and S. K. Wong, Phys. Fluids 28 (1985) 3082.
[10] W. X. Wang, N. Nikajima, M. Okamoto and S. Murakami, Plasma. Phys. Control. Fusion 41 (1999) 1091.
[11] S. Brunner, E. Valeo and J. A. Krommes, Phys. Plasmas 6 (1999) 4504.
[12] X. Q. Xu and M. N. Rosenbluth, Phys. Fluids B 3 (1991) 627.
[13] Z. Lin, M. W. Tang and W. W. Lee, Phys. Plasmas 2 (1995) 2975.
[14] A. M. Dimits and B. I. Cohen, Phys. Rev. E 49 (1994) 709.
[15] H. Sugama, T.-H.Watanabe and M. Nunami, Phys. Plasmas 16 (2009) 112503.
[16] S. Satake, R. Kanno and H. Sugama, Plasma and Fusion Research 3 (2008) S1062.